JBC Papers in Press. Published on August 1, 2012 as Manuscript M112.402727
The latest version is at http://www.jbc.org/cgi/doi/10.1074/jbc.M112.402727

DERP6 (ELP5) and C3ORF75 (ELP6) regulate tumorigenicity and migration of melanoma cells as subunits of Elongator

Pierre Close[*,†,1], Magali Gillard[*,†,1], Aurélie Ladang[*,†], Zheshen Jiang[*,†], Jessica Papuga[*,†], Nicola Hawkes[#], Laurent Nguyen[*,§], Jean-Paul Chapelle[*,†], Fabrice Bouillenne[¶], Jesper Svejstrup[#], Marianne Fillet[*,†,‡] and Alain Chariot[*, †, ∫]

[*]Interdisciplinary Cluster for Applied Genoproteomics (GIGA-R), [†]GIGA Signal Transduction and Laboratory of Medical Chemistry, [§]Developmental Neurobiology Unit and GIGA Neurosciences, [¶]Centre for Protein Engineering, [‡]Laboratory of Analytical Pharmaceutical Chemistry, Department of Pharmacy, CIRM, University of Liège, CHU, Sart-Tilman, B-4000 Liège, Belgium and #Mechanisms of Transcription Laboratory, Cancer Research UK London Research Institute, Clare Hall Laboratories, South Mimms, EN6 3LD, UK, [∫]Walloon Excellence in Life sciences and Biotechnology (WELBIO), GIGA-R, University of Liège, CHU, Sart-Tilman, B-4000 Liege, Belgium

[1]These authors equally contributed to this work

Running title: *Tumorigenicity and migration of melanoma cells require ELP5 and ELP6*

To whom correspondence should be addressed: Drs. Pierre Close and Alain Chariot, Laboratory of Medical Chemistry/GIGA-R, Tour GIGA, +2 B34, CHU Sart-Tilman, 4000 Liège, Belgium, Tel.: +32 4 366 24 72, Fax: +32 4 366 45 34, E-mails: Pierre.Close@ulg.ac.be; Alain.chariot@ulg.ac.be

Keywords: DERP6/ELP5, C3ORF75/ELP6, Elongator, migration, tumorigenesis, melanoma

Background: Elongator is an acetylase complex that regulates cell migration.
Results: DERP6 (ELP5) and C3ORF75 (ELP6) are characterized as Elongator subunits that control cell motility and tumorigenicity of melanoma cells. ELP5 ensures Elongator integrity by connecting ELP3 to ELP4.
Conclusions: ELP5 and ELP6 are new players for migration and tumorigenicity of transformed cells
Significance: Elongator may be involved in both tumor initiation and progression.

ABSTRACT

The Elongator complex is composed of 6 subunits (Elp1-Elp6) and promotes RNAPII transcript elongation through histone acetylation in the nucleus as well as tRNA modification in the cytoplasm. This acetyltransferase complex directly or indirectly regulates numerous biological processes ranging from exocytosis and resistance to heat shock in yeast to cell migration and neuronal differentiation in higher eukaryotes. The identity of human ELP1 through ELP4 has been reported but human ELP5 and ELP6 have remained uncharacterized. Here, we report that DERP6 (ELP5) and C3ORF75 (ELP6) encode these subunits of human Elongator. We further investigated the importance and function of these two subunits by a combination of biochemical analysis and cellular assays. Our results show that DERP6/ELP5 is required for the integrity of Elongator and directly connects ELP3 to ELP4. Importantly, the migration and tumorigenicity of melanoma-derived cells are significantly decreased upon Elongator depletion through ELP1 or ELP3. Strikingly, DERP6/ELP5 and C3ORF75/ELP6-depleted melanoma cells have similar defects, further supporting the idea that DERP6/ELP5 and C3ORF75/ELP6 are essential for Elongator function. Together, our data identify DERP6/ELP5 and C3ORF75/ELP6 as key players for migration, invasion and tumorigenicity of melanoma cells, as integral subunits of Elongator.

The Elongator complex (Elp1-Elp6) was initially identified as a component of a hyper-phosphorylated RNA polymerase II (RNAPII) holoenzyme isolated from budding yeast chromatin and subsequently from human cells (1-4). Elp3, the catalytic subunit, harbours motifs found in the GNAT family of histone acetyltransferases (HATs) (5) and is essential for the ability of Elongator to acetylate histone H3, and to a lesser extent H4, *in vitro* (2,5,6). As a result, yeast *elp3* mutation causes decreased

histone H3 acetylation levels in chromatin *in vivo* (6,7). These data, combined with studies describing the association of Elongator with nascent RNA emanating from elongating RNAPII along the coding region of several yeast genes (8) and with the preferential recruitment of Elongator to the transcribed regions of human genes (9-11), support a role for this complex in transcriptional elongation.

A substantial fraction of Elongator is cytoplasmic (2,12,13), raising the possibility that this complex performs additional molecular functions in the cell (14). In this context, genetic data in yeast demonstrated that Elongator is required for the presence of 5-methoxycarbonylmethyl (mcm^5) and 5-carbamoylmethyl (ncm^5) groups on uridines at the wobble position of some tRNAs (15-17). Although it is still unclear how Elongator precisely acts in the early step of the enzymatic cascade that ultimately generates these correctly modified tRNAs, this function is conserved, at least in *Saccharomyces cerevisiae*, *Caenorhabditis elegans* as well as in *Arabidopsis thaliana* (18,19). Therefore, Elongator may act as a multitasking complex that regulates both transcriptional elongation through histone acetylation in the nucleus as well as translational fidelity through tRNA modifications in the cytoplasm (20). These data undoubtedly demonstrated that Elongator may not only acetylate nuclear histones but also additional and still poorly characterized substrates in the cytoplasm. In agreement with this hypothesis, recent studies indicated that Elongator promotes the acetylation of alpha tubulin in both mice and *Caenorhabditis elegans* (21,22) as well as of the ELKS family member Bruchpilot in *Drosophila* neurons (23).

Loss of function models for Elongator in distinct organisms revealed a variety of cellular processes that rely on this acetylase complex. Indeed, while Elongator yeast mutants (*elp* phenotypes) have slower growth adaptation, temperature sensitivity at 39°C as well as exocytosis, telomeric gene silencing and DNA damage response defects (5,24-26), *Elongata* mutants of *Arabidopsis thaliana* showed impaired root growth due to decreased cell division rate (27). Moreover, deletion of Elp3 in *Drosophila melanogaster* resulted in larval lethality, at least because of an aberrant expression of stress response genes (28). Elongator deficiency is also lethal in mice (29) while migration and differentiation defects were observed in Elp3-depleted cortical neurons during embryogenesis (21). The consequence of impaired Elongator function in humans is exemplified by familial dysautonomia (FD), an autosomal recessive disease characterized by defects in the development and maintenance of autonomic and sensory system neurons (30,31). FD is caused by a mutation in a splice site of the *IKBKAP* gene, which ultimately leads to decreased expression of ELP1, the scaffold protein that assembles Elongator, in a tissue-specific manner (32,33). Interestingly, some ELP3 variants are associated with amyotrophic lateral sclerosis, a progressive motor neuron disease (34), thus strongly suggesting that the Elongator-dependent pathways may be deregulated in distinct neurological disorders (35).

We and others have reported that Elongator critically regulates cell migration, independently of the cell type studied (11,36-38). Indeed, primary or transformed cells depleted for Elongator systematically showed cell motility defects, suggesting that Elongator-dependent protein acetylation plays an important role in cell migration (11,21). It is however still unclear whether and how other Elongator subunits beside ELP1 and ELP3 contribute to this process.

We report here the characterization of Dermal papilla-derived protein 6 (DERP6) and C3ORF75 as human homologues of yeast Elp5 and Elp6, respectively. Moreover, we show that DERP6/ELP5 is essential for Elongator integrity as it connects ELP4 to ELP3. Importantly, ELP5- or ELP6-depleted melanoma-derived cells do not migrate properly and fail to efficiently generate colonies in soft agar, similar to what is observed in ELP1- and ELP3-depleted cells. Wild type DERP6/ELP5, but not a mutant that does not bind ELP1 or ELP3, restores motility in DERP6/ELP5-deficient cells. Taken together, our data identify the genes encoding ELP5 and ELP6 in human cells, define Elongator as a key actor for the tumorigenic potential and motility of melanoma cells, and provide further mechanistic insights into the function of DERP6/ELP5.

EXPERIMENTAL PROCEDURES

Plasmids and antibodies – ORFs encoding human ELP4 and DERP6/ELP5 were cloned into pIRESpuro (Clontech, Palo Alto, CA, USA) with a FLAG tag at the C-terminus. The pCMV-Myc ELP3, FLAG-ELP3 and FLAG-ELP1 expression constructs were

previously described (21). DERP6/ELP5 mutants were generated by PCR and subcloned into the pcDNA3.1 expression vector (Invitrogen). Full length DERP6/ELP5 was also subcloned into the pCMV-Myc expression construct (Clontech). Antibodies used were mouse anti-FLAG, mouse anti-α-tubulin (Sigma Aldrich, St-Louis, MO, USA), rabbit anti-Myc (Santa Cruz, CA, USA) and rabbit anti-Histone H3 (Abcam, Cambridge, UK). The rabbit anti-Elp1, -Elp3, -Elp4, -Elp5 and Elp6 antibodies were previously described (39).

Cell culture, stable cell line establishment – HEK293 cells were cultured as previously described (40). The mouse melanoma-derived B16-F10-luc-G5 Bioware cells (Caliper LifeSciences, Hopkinton, MA, USA) were maintained in DMEM supplemented with 10% foetal bovine serum, 1% antibiotics, 1% L-glutamine and G418. To generate HEK293 stably expressing ELP4- or DERP6/ELP5-FLAG proteins, cells were transfected with the relevant pIRESpuro construct and selected in 1µg/ml puromycin (Sigma Aldrich). Cells were maintained in selecting media for 3 weeks and surviving cells used for experiment after transgene expression was checked.

Subcellular fractionation – HEK293 cells were divided into cytoplasmic and nuclear fractions as previously described (41). Briefly, cells were trypsinized, washed in PBS, and lyzed in cytoplasmic lysis buffer (10mM Tris HCl pH 7.9, 340mM sucrose, 3mM $CaCl_2$, 2mM $Mg(OAc)_2$, 0.1mM EDTA, 1mM DTT, 0.5% NP40, protease inhibitors). Nuclei were pelleted by centrifugation at 3,500g for 15min, washed in cytoplasmic lysis without NP40 and lyzed in nuclear lysis buffer (20mM Hepes pH 7.9, 250mM KOAc, 1% SDS, 1mM DTT, protease inhibitors). For ease of comparison, equal proportion of cytoplasmic or nuclear fractions was loaded on SDS-page gel.

Lentiviral Cell Infections – Control shRNA as well as shRNA Elp1, -Elp3, -Elp5 and -Elp6 lentiviral constructs were purchased from Sigma Aldrich. The corresponding sequences are listed in the Supplementary Table 1. Lenti-X 293T cells (Clontech) were transfected with VSV-G, gag and pol expressing constructs as well as with the vector (pLKO.1-puro) containing the shRNA sequence of interest. Infectious supernatants were collected 48-52 hours post-transfection, and cleared by centrifugation. Polybrene was added (5µg/ml), and the cleared supernatants were used to transduce B16-F10 or HEK293 cells. Infected cells were maintained in puromycin-containing media to produce stable knock down cells. The efficiency of the RNA interference was validated by either western blot or qRT-PCR analysis.

Purification and identification of human Elongator complex from cytoplasmic fractions – 10^8 cells stably expressing ELP4-FLAG were lysed with cytoplasmic lysis buffer (10mM Tris HCl pH 7.9, 340mM sucrose, 3mM $CaCl_2$, 2mM $Mg(OAc)_2$, 0.1mM EDTA, 1mM DTT, 0.5% NP40, protease inhibitors). Nuclei were then pelleted by centrifugation at 3,500*g* for 15 min and discarded. The cytoplasmic fraction was further cleared by centrifugation at 20,000g for 30 min and the supernatant was collected. For negative control purification, the same extracts were prepared from the same amount of untagged cells. The sample was then applied to M2 agarose beads (Sigma Aldrich) and incubated for 4h at 4°C. After binding, beads were washed extensively with washing buffer (20mM Hepes pH 7.9, 250mM KOAc, 1% Triton X-100, 10% glycerol, 3mM EDTA, 1mM DTT, protease inhibitors). Finally, proteins were eluted by using FLAG elution buffer (20mM Hepes pH 7.9, 100mM KOAc, 3mM EDTA, 1mM DTT, 200 µg/ml 3xFLAG peptide, protease inhibitors). Eluates were resolved by 4-12% bis-Tris gradient SDS-PAGE and analyzed by Sypro Ruby staining (Invitrogen). In-gel digestion of each band was then performed by addition of modified trypsin (Promega, Madison, WI) in 50mM ammonium bicarbonate at 37°C overnight and further analyzed by LC-Chip nano high performance liquid chromatography (HPLC) electrospray MS-MS using an XCT iontrap mass spectrometer (Agilent, Santa Clara, CA). The HPLC separations were performed on an RP C18 Zorbax column from Agilent. The mobile phase was a 60 min gradient mixture formed as follows: mixture A, water-acetonitrile-formic acid (97/3/0.1 [vol/vol/vol]); mixture B, acetonitrile-water-formic acid (90/10/0.1 [vol/vol/vol]). The flow rate was fixed at 300 nL/min. The collision energy was set automatically depending on the mass of the parent ion. Each MS full scan was followed by MS-MS scans of the first four most intense peaks detected in the prior MS scan. A list of peptide masses was subsequently introduced into the database for protein identification searches using MASCOT (Matrix Sciences). For size exclusion chromatography, samples were loaded on superdex 200 in buffer A (20mM Hepes-KOH,

0.01% NP40, 10% glycerol, 250mM KOAc). 250 µl fractions were collected, and sizes were estimated by running protein size markers (Biorad) in parallel.

Immunoprecipitations and Immunofluorescences – Immunoprecipitations involving ectopically expressed proteins were conducted as previously described (40). For immunostainings, HEK293 cells were washed twice in PBS, fixed in 4% PFA for 20 min at room temperature and washed three times in washing buffer (PBS, 0.1% Tween). Cells were subsequently permeabilized in PBS supplemented with 0.5% Triton X-100 for 15 min, incubated in a blocking buffer containing PBS, 0.3% Triton X-100 and 5% Donkey Serum for 30 min at room temperature and then incubated with primary antibodies for 1 hour. After three washes in the blocking buffer, cells were incubated with Alexa546- (Invitrogen) or FITC- (Jackson Immunoresearch Laboratories, West Grove, PA, USA) conjugated secondary antibodies in the same buffer for 1 hour at room temperature and subsequently washed three times. Cells were counterstained with To-Pro (Invitrogen), washed once and mounted in ProLong Gold antifade reagent (Invitrogen) between slide and coverslip. Images were acquired with a Leica TCS SP2 confocal (objective 63x with oil immersion).

Wound healing, soft agar colony and 3D cell culture assays – Wound healing assays were conducted as previously described (11). Briefly, $3x10^5$ B16-F10 cells expressing shCTR, shElp1, -3, -5 or -6 were seeded in 24-well plates in triplicates. The next day, cells were treated with Mitomycin C (1 µg/ml) for two hours before performing a linear scratch in the confluent cell monolayer. For each well, one picture was taken at time 0 (just after the scratch) and after 6 or 7 hours. Cells were imaged using a Nikon Eclipse TS100 phase-contrast microscope equipped with a 10x objective. For soft agar assays, $2x10^3$ B16-F10 cells expressing shCTRL, shElp1,-3, -5 or -6 lentiviral constructs were plated in 6-well plates in triplicates in culture media containing 0.4% agar on top of media containing 0.8% agar. Cells were incubated for 2 weeks and culture media was replaced every 2-3 days. At the end of the experiment, macroscopic colonies were stained with crystal violet 0.005% and scored with the ImageJ sofware. 3D cell culture assays were carried out mainly as described (42). Briefly, type I collagen from rat tail (a generous gift from A. Colige, Laboratory of Connective Tissues Biology, GIGA Cancer, University of Liege, Belgium) was diluted to a concentration of 2mg/ml and the pH was neutralized by adding 1:3 volume of DMEM. 800µl aliquots were immediately added to 12-well culture plates and incubated at 37°C until gelation occurred. A drop of collagen containing $2x10^5$ control or Elp1-depleted cells was added on top of solidified collagen. After 30 min incubation at 37°C, overlying collagen gels were generated. Wells were then filled with culture media and incubated for 3 weeks at 37°C. The culture media was replaced every 2-3 days. Satellites colonies were stained using a solution of 0.2% methylene blue in 50% methanol and imaged with a Canon camera.

Statistical analysis – Comparison between 2 groups was carried out by doing Student t-tests. Significance was reached when $p<0.1$ '*', $p<0.05$ '**', $p<0.01$ '***'.

RESULTS

Identification of DERP6 and C3ORF75 as Elongator subunits – Human Elongator was previously purified from HeLa cells, which led to the identification of ELP1, ELP2 and ELP3 as subunits of the so-called "core" complex (2,12). Elongator also exists as a larger six-subunit complex referred to as the "holo-complex" that has HAT activity and includes ELP4 as well as two uncharacterized polypeptides, namely p38 (ELP5) and p30 (ELP6) (12). These products are likely to be encoded by one of the several homologues of yeast *elp5* and *elp6* in human cells, but their identity has not been reported. In order to identify the p38 and p30 proteins, we generated HEK293 cells stably expressing FLAG-tagged ELP4, and used it as a bait to purify human Elongator (Fig. 1A). Eluted proteins were subjected to SDS-PAGE analysis and bands were identified by mass spectrometry (MS) (see Supplementary Figs. 1 and 2) (43). They included ELP1, ELP2, ELP3, ELP4 as well as two products, namely DERP6 and C3ORF75, whose apparent molecular weights (38 and 30 kDa, respectively), matched that of the uncharacterized subunits of human Elongator (Fig. 1A, lane 2) (12). Sequence alignment confirmed that DERP6 and C3ORF75 correspond to human homologues of yeast Elp5 and Elp6, respectively (Supplementary Figs. 3 and 4).

To further substantiate the notion that DERP6 and C3ORF75 are part of the human Elongator complex, we established a stable cell

line expressing FLAG-tagged DERP6/ELP5 and applied the same purification protocol. DERP6/ELP5-FLAG co-immunoprecipitated endogenous ELP1, ELP3, ELP4 as well as C3ORF75/ELP6 (Fig. 1B and 1C). Endogenous ELP4 immunoprecipitation also brought down DERP6/ELP5-FLAG (Fig. 1D). Moreover, ELP1, ELP3, ELP4 and DERP6/ELP5-FLAG co-eluted as a 600 kDa complex on gel filtration analysis, as previously described (1,45) (Fig. 1E). We next performed immunofluorescence analysis in order to determine DERP6/ELP5 subcellular localization. Ectopically expressed ELP1 and ELP3 were mainly, but not exclusively, located in the cytoplasm, as previously described (Fig. 2A) (3,21,36,46). ELP4 and DERP6/ELP5 were also mainly found in this cell compartment, showing that holo-Elongator subunits colocalize. In agreement with our immunofluorescence data, western blot analysis performed on cytoplasmic versus nuclear fractions of HEK293 cells indicated that DERP6/ELP5-FLAG was mostly found in the cytoplasm (Fig. 2B, top panel, lane 1). About 14% of this protein was nevertheless detected in the nucleus of those cells (Fig. 2B, top panel, lane 2). Taken together, these data indicate that DERP6 and C3ORF75 are part of the Elongator complex, as human homologues of yeast Elp5 and Elp6. We therefore renamed these two proteins ELP5 and ELP6.

Elongator-deficient melanoma cells have motility defects – We previously reported that Elongator-depleted HeLa cells display migration defects, at least partly due to a failure to properly express genes coding for proteins involved in cell motility (11). To explore whether Elongator also regulates cell migration in melanomas, we first generated B16-F10 cells deficient for Elp1 through lentivirus based RNA interference using two distinct sequences targeting the Elp1 transcript, or a control sequence ("shRNA Elp1#1", shRNA Elp1#2" and "shRNA control (CTR)", respectively). Elp1 was efficiently depleted, as judged by western blot analysis (Fig. 3A, top panel), which led to the destabilization of the Elp3 protein, as previously shown (11,39) (Fig. 3A, middle panel). The migrating capacity of these cells was assessed by wound healing assay. Significant closure of the gaps in cell monolayers had occurred after 7 hours in control B16-F10 cells, whereas a clear delay was observed in Elp1-depleted cells, independently of the sequence used to target the Elp1 transcript (Fig. 3B). We next generated Elp3-depleted B16-F10 cells using the same experimental approach (Fig. 3C) and subjected them to wound healing assays. Elp3 deficiency in B16-F10 cells caused a significant delay in wound healing as well (Fig. 3D). Importantly, ELP3 expression in these cells restored their migration potential (Fig. 3E). These data suggest that both Elp1 and Elp3 Elongator subunits control cell migration in melanoma-derived cells.

Elongator is essential for anchorage-independent growth and invasive potential of melanoma-derived cells – Wound healing assays are used to assess the migrating capacity of any cell type, but this assay does not address the question of tumorigenesis. To determine whether Elongator regulates this latter process, we subsequently assessed the anchorage-independent growth of control-, Elp1- or Elp3-depleted B16-F10 cells by counting colonies able to grow in soft agar. This cellular assay is widely used to study tumorigenic potential of cells. Whereas control B16-F10 cells efficiently generated colonies, Elp1 or Elp3 deficiency dramatically impaired the capacity of melanoma-derived cells to growth in an anchorage-independent manner (Fig. 4A and B, respectively).

To address the issue of tumour invasion and expansion through the extracellular matrix, we used three-dimensional (3D) cell culture systems (47). Briefly, this experimental approach is based on the growth of invasive cancer cells in collagen matrices, and the production of satellite colonies generated from the primary cancer cells. Consequently, key steps of the metastatic process are recapitulated including cell motility and invasion, expansion through a collagen matrix as well as cell survival at distant sites (42). We investigated to which extent satellite colony formation of melanoma-derived cells required Elongator. As expected, control B16-F10 cells generated multiple satellite colonies, a property that was dramatically affected in Elp1-depleted cells (Fig. 4C). Taken together, our data indicate that Elongator is crucial for transformation as well as for the invasive potential of melanoma-derived cells.

Elp5 and Elp6 regulate cell migration and tumorigenesis as Elongator subunits – As ELP5 and ELP6 were identified as Elongator subunits, we next examined whether these proteins also regulate cell migration. Elp5 or Elp6 were efficiently depleted from B16-F10 cells, as judged by the dramatic decrease in their corresponding mRNA levels in cells infected

with two distinct shRNA constructs (Fig. 5A and 5C). Moreover, Elp5- or Elp6-depleted cells also showed cell motility defects, as evidenced by the significant delay in wound healing observed compared to control cells, independently of the shRNA sequence used to deplete them (Fig. 5B and 5D, respectively T6h). Finally, Elp5- or Elp6-deficient B16-F10 cells also showed strong defects in their capacity to form colonies in soft agar (Fig. 5E and 5F, respectively).

Having established the role of Elp5 and Elp6 in cell migration, we next explored the structure-function relationship of the Elp5 protein. We generated a variety of ELP5 mutants lacking N- or C- terminal amino acids ("ΔN50, ΔN100, ΔN150 as well as ΔC50, ΔC100 and ΔC150 ELP5", respectively) (Fig. 6A). These mutants were subsequently tested for their ability to bind other Elongator subunits in co-immunoprecipitation experiments. While the ΔC50 mutant remained capable of binding endogenous ELP4, the ΔN50 ELP5 mutant failed to do so, suggesting that the first 50 amino acids are required for the interaction of ELP5 with ELP4 (Fig. 6B, to panel, compare lanes 2, 3 and 6, respectively). The ΔC100 ELP5 mutant also failed to efficiently bind ELP4, which might suggest that ELP5 harbours a second ELP4-interacting domain between amino acids 216 and 265 (Fig. 6B, top panel, compare lanes 2 and 7). Interestingly, despite its inability to bind ELP4, the ΔN50 ELP5 mutant still bound endogenous ELP1, or ectopically expressed ELP3, as did the ΔC100 mutant, suggesting that ELP5 binds ELP4 and ELP3 (or ELP1) through distinct domains (Fig. 6C, top and second panel from the top, lanes 4 and 8). Deletion of 150 N-terminal or C-terminal amino acids was required to disrupt the interaction of ELP5 with ELP3 and ELP1 (Fig. 6C, top panel and second panel from the top, lanes 6 and 9). Finally, as the ΔN150 ELP5 mutant failed to bind any of the tested Elongator subunits, we checked whether this product would efficiently restore cell migration when expressed in Elp5-depleted cells. Both full-lengh ELP5 and the ΔN150 mutant were detected by western blot analysis using extracts collected at the end of the wound healing analysis (Fig. 6D, lanes 3 and 4). Interestingly, however, while full-length ELP5 completely restored the migration potential of these cells, the ΔN150 mutant failed to do so (Fig. 6D). Therefore, these results show that ELP5 regulates cell motility as a subunit of Elongator.

ELP5 connects ELP4 to ELP3 – To learn more on the molecular mechanisms by which ELP5 is required for the activity of the Elongator complex, we experimentally assessed the interaction network of Elongator subunits in presence or absence of ELP5. As expected, endogenous ELP1 and ELP3 could be detected in an ELP4-FLAG pull down (Fig. 7A, top panel and second panel from the top, lanes 3). However, whereas ELP1 could efficiently bind ELP4 in ELP5-depleted HEK293 cells, ELP3-ELP4 interaction required ELP5, indicating that ELP5 connects ELP4 to ELP3 (Fig. 7A, top and second panel from the top, compare lanes 3 and 4). To validate these results, we immunoprecipitated FLAG-ELP3 from control or ELP5-depleted HEK 293 cells and observed that though endogenous ELP1 was detectable in the immunoprecipitates in both experimental conditions (Fig. 7B, top panel compare lanes 3 and 4), ELP4-ELP3 was decreased in the absence of ELP5 (Fig. 7B, third panel from the top, compare lanes 3 and 4). Therefore, ELP5 is dispensable for the interaction between ELP3 and ELP1 but is required for optimal binding of ELP3 to ELP4.

DISCUSSION

We report here the identification of two previously uncharacterized human Elongator subunits, namely DERP6/ELP5 and C3ORF75/ELP6. We show that both proteins control cell migration in melanoma-derived cells and provide evidences that ELP5 fulfills this function at least partly by connecting ELP3 to ELP4. Our results also point to a role of Elongator in regulating the growth of transformed cells in an anchorage-independent manner. Our data further demonstrate that ELP1-ELP6 act as integral Elongator subunits to control cell motility and tumorigenicity of transformed cells and provide additional insights into the structure-function of this acetylase complex.

Elongator is unique, as it includes two sub-complexes, namely the core-elongator (ELP1, 2 and 3) that has the acetyltransferase activity and the ELP456 subcomplex, which has recently been described as an hexameric RecA-like ATPase in yeast (48,49). Only very recent studies actually started to explore the structure-function relationship of Elongator. In yeast, deletion of any of the (*ELP*) genes encoding the 6 subunits confers similar phenotypes, yet Elp2 deletion does not seem to impair Elongator

integrity *in vitro* (6,50). On the other hand, ELP3 is strongly destabilized in the absence of ELP1, thus defining this latter subunit as a crucial actor for assembling Elongator into a functional complex in yeast but also in human cells (11,39). Beside a C-terminal HAT domain, yeast Elp3 also harbors an N-terminal iron-sulfur (FeS) cluster motif with no described catalytic activity but critical for the association of Elongator with accessory factors such as Kti11 and Kti12 (51).

Here, we show that ELP5 constitutively binds ELP1 and ELP3 and also connects ELP3 to ELP4. Our data suggest that this role underlies its ability to ensure Elongator integrity and function. We demonstrated that ELP5 bound ELP1/ELP3 through two distinct domains, namely a N-terminal motif spanning from amino acids 101 and 150 as well as a second motif from amino acids 166 to 216. It also binds ELP4 through amino acids 1 to 50 and also through amino acids 217 to 266 (Figs. 6B and 6C). Interestingly, the very C-terminal region of ELP5 that is highly conserved throughout evolution is clearly located downstream of the ELP1/3-interacting domain while the motif required for binding to ELP4 only partially includes the most conserved residues. Indeed, the last 50 amino acids of ELP5 are dispensable for the interaction with ELP1/3 and 4, yet they include numerous conserved residues, which may indicate that ELP5 fulfills key functions that go beyond its capacity to connect Elongator subunits. A recent study performed in yeast defined amino acids E61 and D107 of Elp5 as critical residues for ATPase enzymatic activity (48). Surprisingly, these residues as well as their flanking sequences are poorly conserved throughout evolution (Supplementary Fig. 3). Therefore, future work is needed to confirm whether this enzymatic activity can also be detected in human ELP5 and to examine to what extent this activity contributes to the capacity of ELP5 to promote cell migration.

Our report provides key insights into the biological functions of DERP6, a protein previously described as a positive regulator of the p53-dependent pathways (44). We previously showed that Elongator deficiency actually slightly stabilized p53 in colon cancer-derived HCT116 cells, but that it did not impair DNA damage-induced p53 phosphorylation (52). We also demonstrated that some p53 target genes were aberrantly expressed upon Elongator deficiency, which indicated that this acetylase complex protects cells from an inappropriate expression of p53-dependent genes rather than promoting p53 activation. Furthermore, we did not observe significant change in p53 levels upon Elp5 depletion (data not shown). Finally, a recent study in *Drosophila* pointed out for a role of Elongator as positive regulator of the insulin-receptor-TOR signaling, which ultimately control cell growth and cell death. Indeed, mutations in the *poly* gene (encoding the Elp6 homologue in *Drosophila*) led to increased apoptotic cell death in larvae (53). In support to this hypothesis, Elongator deficiency is linked to FD, a neurodevelopmental and neurodegenerative genetic disorder in which premature or excessive cell death is observed. Even if it is currently unclear whether the progression of this disease involves a deregulated p53 response, it provides enough evidence for Elongator acting as a negative, rather than a positive regulator of p53.

We show here that Elp1-, Elp3-, Elp5- and Elp6-deficient melanoma-derived cells do not efficiently form colonies in soft agar. Therefore, Elongator is a protein complex that promotes cell growth and/or survival in an anchorage-independent. The molecular mechanisms by which Elongator is involved in this process are however not known. Based on the role of this acetylase complex in tumorigenesis but also in the migration of melanoma-derived cells, it is tempting to speculate that tumor initiation but also tumor progression may both rely on Elongator. The potential contribution of each subunit of this acetylase complex in both processes is currently under investigation.

REFERENCES

1. Otero, G., Fellows, J., Li, Y., de Bizemont, T., Dirac, A. M., Gustafsson, C. M., Erdjument-Bromage, H., Tempst, P., and Svejstrup, J. Q. (1999) *Mol Cell* **3**, 109-118
2. Kim, J. H., Lane, W. S., and Reinberg, D. (2002) *Proc Natl Acad Sci U S A* **99**, 1241-1246
3. Hawkes, N. A., Otero, G., Winkler, G. S., Marshall, N., Dahmus, M. E., Krappmann, D., Scheidereit, C., Thomas, C. L., Schiavo, G., Erdjument-Bromage, H., Tempst, P., and Svejstrup, J. Q. (2002) *J Biol Chem* **277**, 3047-3052
4. Krogan, N. J., and Greenblatt, J. F. (2001) *Mol Cell Biol* **21**, 8203-8212
5. Wittschieben, B. O., Otero, G., de Bizemont, T., Fellows, J., Erdjument-Bromage, H., Ohba, R., Li, Y., Allis, C. D., Tempst, P., and Svejstrup, J. Q. (1999) *Mol Cell* **4**, 123-128
6. Winkler, G. S., Kristjuhan, A., Erdjument-Bromage, H., Tempst, P., and Svejstrup, J. Q. (2002) *Proc Natl Acad Sci U S A* **99**, 3517-3522
7. Kristjuhan, A., Walker, J., Suka, N., Grunstein, M., Roberts, D., Cairns, B. R., and Svejstrup, J. Q. (2002) *Mol Cell* **10**, 925-933
8. Gilbert, C., Kristjuhan, A., Winkler, G. S., and Svejstrup, J. Q. (2004) *Mol Cell* **14**, 457-464
9. Metivier, R., Penot, G., Hubner, M. R., Reid, G., Brand, H., Kos, M., and Gannon, F. (2003) *Cell* **115**, 751-763
10. Kouskouti, A., and Talianidis, I. (2005) *Embo J* **24**, 347-357
11. Close, P., Hawkes, N., Cornez, I., Creppe, C., Lambert, C. A., Rogister, B., Siebenlist, U., Merville, M. P., Slaugenhaupt, S. A., Bours, V., Svejstrup, J. Q., and Chariot, A. (2006) *Mol Cell* **22**, 521-531
12. Hawkes, N. A., Otero, G., Winkler, G. S., Marshall, N., Dahmus, M. E., Krappmann, D., Scheidereit, C., Thomas, C. L., Schiavo, G., Erdjument-Bromage, H., Tempst, P., and Svejstrup, J. Q. (2002) *J Biol Chem* **277**, 3047-3052
13. Holmberg, C., Katz, S., Lerdrup, M., Herdegen, T., Jaattela, M., Aronheim, A., and Kallunki, T. (2002) *J Biol Chem* **277**, 31918-31928
14. Svejstrup, J. Q. (2007) *Curr Opin Cell Biol* **19**, 331-336
15. Huang, B., Johansson, M. J., and Bystrom, A. S. (2005) *RNA* **11**, 424-436
16. Esberg, A., Huang, B., Johansson, M. J., and Bystrom, A. S. (2006) *Mol Cell* **24**, 139-148
17. Bauer, F., Matsuyama, A., Candiracci, J., Dieu, M., Scheliga, J., Wolf, D. A., Yoshida, M., and Hermand, D. (2012) *Cell Rep* **1**, 424-433
18. Mehlgarten, C., Jablonowski, D., Wrackmeyer, U., Tschitschmann, S., Sondermann, D., Jager, G., Gong, Z., Bystrom, A. S., Schaffrath, R., and Breunig, K. D. (2010) *Mol Microbiol* **76**, 1082-1094
19. Chen, C., Tuck, S., and Bystrom, A. S. (2009) *PLoS genetics* **5**, e1000561
20. Versees, W., De Groeve, S., and Van Lijsebettens, M. (2010) *Mol Microbiol* **76**, 1065-1069
21. Creppe, C., Malinouskaya, L., Volvert, M. L., Gillard, M., Close, P., Malaise, O., Laguesse, S., Cornez, I., Rahmouni, S., Ormenese, S., Belachew, S., Malgrange, B., Chapelle, J. P., Siebenlist, U., Moonen, G., Chariot, A., and Nguyen, L. (2009) *Cell* **136**, 551-564
22. Solinger, J. A., Paolinelli, R., Kloss, H., Scorza, F. B., Marchesi, S., Sauder, U., Mitsushima, D., Capuani, F., Sturzenbaum, S. R., and Cassata, G. (2010) *PLoS genetics* **6**, e1000820

23. Miskiewicz, K., Jose, L. E., Bento-Abreu, A., Fislage, M., Taes, I., Kasprowicz, J., Swerts, J., Sigrist, S., Versees, W., Robberecht, W., and Verstreken, P. (2011) *Neuron* **72**, 776-788
24. Rahl, P. B., Chen, C. Z., and Collins, R. N. (2005) *Mol Cell* **17**, 841-853
25. Chen, C., Huang, B., Eliasson, M., Ryden, P., and Bystrom, A. S. (2011) *PLoS genetics* **7**, e1002258
26. Li, Q., Fazly, A. M., Zhou, H., Huang, S., Zhang, Z., and Stillman, B. (2009) *PLoS genetics* **5**, e1000684
27. Nelissen, H., Fleury, D., Bruno, L., Robles, P., De Veylder, L., Traas, J., Micol, J. L., Van Montagu, M., Inze, D., and Van Lijsebettens, M. (2005) *Proc Natl Acad Sci U S A* **102**, 7754-7759
28. Walker, J., Kwon, S. Y., Badenhorst, P., East, P., McNeill, H., and Svejstrup, J. Q. (2011) *Genetics* **187**, 1067-1075
29. Chen, Y. T., Hims, M. M., Shetty, R. S., Mull, J., Liu, L., Leyne, M., and Slaugenhaupt, S. A. (2009) *Mol Cell Biol* **29**, 736-744
30. Slaugenhaupt, S. A., and Gusella, J. F. (2002) *Curr Opin Genet Dev* **12**, 307-311
31. Gold-von Simson, G., and Axelrod, F. B. (2006) *Curr Probl Pediatr Adolesc Health Care* **36**, 218-237
32. Anderson, S. L., Coli, R., Daly, I. W., Kichula, E. A., Rork, M. J., Volpi, S. A., Ekstein, J., and Rubin, B. Y. (2001) *Am J Hum Genet* **68**, 753-758
33. Slaugenhaupt, S. A., Blumenfeld, A., Gill, S. P., Leyne, M., Mull, J., Cuajungco, M. P., Liebert, C. B., Chadwick, B., Idelson, M., Reznik, L., Robbins, C., Makalowska, I., Brownstein, M., Krappmann, D., Scheidereit, C., Maayan, C., Axelrod, F. B., and Gusella, J. F. (2001) *Am J Hum Genet* **68**, 598-605
34. Simpson, C. L., Lemmens, R., Miskiewicz, K., Broom, W. J., Hansen, V. K., van Vught, P. W., Landers, J. E., Sapp, P., Van Den Bosch, L., Knight, J., Neale, B. M., Turner, M. R., Veldink, J. H., Ophoff, R. A., Tripathi, V. B., Beleza, A., Shah, M. N., Proitsi, P., Van Hoecke, A., Carmeliet, P., Horvitz, H. R., Leigh, P. N., Shaw, C. E., van den Berg, L. H., Sham, P. C., Powell, J. F., Verstreken, P., Brown, R. H., Jr., Robberecht, W., and Al-Chalabi, A. (2009) *Hum Mol Genet* **18**, 472-481
35. Nguyen, L., Humbert, S., Saudou, F., and Chariot, A. (2010) *Trends Mol Med* **16**, 1-6
36. Johansen, L. D., Naumanen, T., Knudsen, A., Westerlund, N., Gromova, I., Junttila, M., Nielsen, C., Bottzauw, T., Tolkovsky, A., Westermarck, J., Coffey, E. T., Jaattela, M., and Kallunki, T. (2008) *J Cell Sci* **121**, 854-864
37. Boone, N., Loriod, B., Bergon, A., Sbai, O., Formisano-Treziny, C., Gabert, J., Khrestchatisky, M., Nguyen, C., Feron, F., Axelrod, F. B., and Ibrahim, E. C. (2010) *PLoS One* **5**, e15590
38. Lee, G., Papapetrou, E. P., Kim, H., Chambers, S. M., Tomishima, M. J., Fasano, C. A., Ganat, Y. M., Menon, J., Shimizu, F., Viale, A., Tabar, V., Sadelain, M., and Studer, L. (2009) *Nature* **461**, 402-406
39. Petrakis, T. G., Wittschieben, B. O., and Svejstrup, J. Q. (2004) *J Biol Chem* **279**, 32087-32092
40. Viatour, P., Dejardin, E., Warnier, M., Lair, F., Claudio, E., Bureau, F., Marine, J. C., Merville, M. P., Maurer, U., Green, D., Piette, J., Siebenlist, U., Bours, V., and Chariot, A. (2004) *Mol Cell* **16**, 35-45
41. Close, P., East, P., Dirac-Svejstrup, A. B., Hartmann, H., Heron, M., Maslen, S., Chariot, A., Soding, J., Skehel, M., and Svejstrup, J. Q. (2012) *Nature* **484**, 386-389
42. Gobeil, S., Zhu, X., Doillon, C. J., and Green, M. R. (2008) *Genes Dev* **22**, 2932-2940
43. Sebastiaan Winkler, G., Lacomis, L., Philip, J., Erdjument-Bromage, H., Svejstrup, J. Q., and Tempst, P. (2002) *Methods* **26**, 260-269

44. Yuan, J., Tang, W., Luo, K., Chen, X., Gu, X., Wan, B., and Yu, L. (2006) *Molecular biology reports* **33**, 151-158
45. Winkler, G. S., Petrakis, T. G., Ethelberg, S., Tokunaga, M., Erdjument-Bromage, H., Tempst, P., and Svejstrup, J. Q. (2001) *J Biol Chem* **276**, 32743-32749
46. Pokholok, D. K., Hannett, N. M., and Young, R. A. (2002) *Mol Cell* **9**, 799-809
47. Doillon, C. J., Gagnon, E., Paradis, R., and Koutsilieris, M. (2004) *Anticancer Res* **24**, 2169-2177
48. Glatt, S., Letoquart, J., Faux, C., Taylor, N. M., Seraphin, B., and Muller, C. W. (2012) *Nature structural & molecular biology* **19**, 314-320
49. Lin, Z., Zhao, W., Diao, W., Xie, X., Wang, Z., Zhang, J., Shen, Y., and Long, J. (2012) *J Biol Chem* **287**, 21501-21508
50. Fellows, J., Erdjument-Bromage, H., Tempst, P., and Svejstrup, J. Q. (2000) *J Biol Chem* **275**, 12896-12899
51. Greenwood, C., Selth, L. A., Dirac-Svejstrup, A. B., and Svejstrup, J. Q. (2009) *J Biol Chem* **284**, 141-149
52. Cornez, I., Creppe, C., Gillard, M., Hennuy, B., Chapelle, J. P., Dejardin, E., Merville, M. P., Close, P., and Chariot, A. (2008) *Biochem Pharmacol* **75**, 2122-2134
53. Bolukbasi, E., Vass, S., Cobbe, N., Nelson, B., Simossis, V., Dunbar, D. R., and Heck, M. M. (2012) *Open Biology Journal* **2**, 110031
54. Li, Y., Takagi, Y., Jiang, Y., Tokunaga, M., Erdjument-Bromage, H., Tempst, P., and Kornberg, R. D. (2001) *J Biol Chem* **276**, 29628-29631

Acknowledgements – The authors are grateful to the GIGA Imaging facility for immunofluorescence analysis and to Charles Lambert, Audrey Hoffmann and Alain Colige (GIGA Cancer, University of Liege, Belgium) for providing collagen. P.C., L.N. and A.C. are Senior Research Assistant, Research Associate and Senior Research Associate at the Belgian National Funds for Scientific Research ("F.N.R.S."), respectively whereas M.G., A.L. and Z.J. are beneficiary of a TELEVIE PhD fellowship. This work was supported by grants from the F.N.R.S. the Belgian Federation against cancer, the Concerted Research Action Program (11/16-01, University of Liege), the "Centre Anti-Cancéreux ", the "Leon Frédéricq" Foundation (Faculty of Medicine, University of Liege), the Inter-University Attraction Pole 6/12 (Federal Ministery of Science) and the King Baudouin Foundation (Brussels, Belgium). Work in the Svejstrup Lab was supported by a generous in-house grant from Cancer research UK.

FIGURE LEGENDS

Figure 1: Identification of DERP6 and C3ORF75 as Elongator subunits. A. Elongator was purified from the cytoplasmic fraction of ELP4-FLAG expressing cells. Equal amount of the M2 chromatography eluates from Mock (M) and ELP4-FLAG (E) were separated by 4-12% SDS-PAGE and stained with Sypro Ruby. Bands were extracted and analysed by mass spectrometry. Arrows indicate the co-eluting Elongator subunits as well as Hsp70, α- and β-tubulin (* shows non-specific bands). **B.** Western blot analysis of M2 eluates from control (Mock) or DERP6/ELP5-FLAG expressing cells. Proteins were detected with antibodies as shown on the left. **C**. Anti-ELP6 western blot analysis on anti-FLAG immunoprecipitates from control or DERP6/ELP5-FLAG expressing cells (top panel). At the bottom, anti-ELP5 western blot performed on the crude cell extracts (input). **D.** Endogenous ELP4 was immunoprecipitated from Mock or DERP6/ELP5-FLAG expressing cells and proteins detected with antibodies listed on the right. **E.** The M2-purified Elongator complex from (B) was analyzed by size exclusion chromatography. Vo is the void volume fraction. Proteins were detected by western blotting using the antibodies indicated on the left.

Figure 2: ELP1, ELP3, ELP4 and ELP5 are mainly cytoplasmic. A. HEK293 cells were transfected with the indicated expression plasmids and immunofluorescence analysis were conducted using anti-Myc or -FLAG antibodies (left column). To-Pro (blue) was used to visualize the nuclei (middle and right columns). **B**. DERP6/ELP5-FLAG was transfected in HEK293 cells and cytoplasmic versus nuclear extracts (C and N, respectively) were isolated from the resulting cells. Those extracts were subjected to anti-FLAG, -α-tubulin and -Histone H3 (cytoplasmic and nuclear markers, respectively), as indicated. A quantification of the cellular distribution of DERP6/ELP5 is illustrated as well.

Figure 3: Elp1 and Elp3 regulate cell motility of melanoma-derived B16-F10 cells. A. Generation and characterization of Elp1-deficient B16-F10 cells. Anti-Elp1, -Elp3 and -α-tubulin (loading control) western blot analysis were carried out using cell extracts from B16-F10 infected with lentiviral constructs delivering small hairpin RNAs targeting two distinct sequences of the Elp1 transcript, or a control sequence as a negative control ("shRNA Elp1#1", "shRNA Elp1#2" and "shRNA control (CTR)", respectively). **B**. Migration of control (CTR) or Elp1-depleted (Elp1#1 or Elp1#2) melanoma-derived cells was measured by wound healing assay. Pictures were taken at the indicated times after the wound. A quantification of the data obtained is illustrated on the right. For each experimental condition, the width of the wound was set to 100% at time 0 and the width in other time points expressed relative to that. The figure shows the data from a representative experiment performed in triplicates (mean values ± S.D.). **C**. Generation and characterization of Elp3-depleted melanoma-derived cells. mRNA levels from B16-F10 cells infected with lentiviral constructs delivering small hairpin RNAs targeting two distinct sequences of the Elp3 transcript, or a control sequence ("shRNA Elp3#1", "shRNA Elp3#2" and "shRNA CTR", respectively), were assessed by qRT-PCR. Elp3 mRNA levels in control B16-F10 cells were set to 100%, and mRNA levels in other experimental conditions are relative to that. The figure shows the data from a representative experiment performed in triplicates (mean values ± S.D.). **D**. same as B, but using Elp3-depleted melanoma-derived generated in C. **E**. Wound healing assays were conducted with shRNA control, shRNA Elp3 B16-F10 cells or with shRNA Elp3 B16-F10 cells transfected with full length Myc-ELP3. A quantification of the data obtained is illustrated on the right. For each experimental condition, the width of the wound was set to 100% at time 0 and the width in other time points expressed relative to that. The figure shows the data from a representative experiment performed in triplicates (mean values ± S.D.). On the left, anti-Myc western blots were carried out with protein extracts from the indicated cells collected at the end of the wound healing assay. "Mock" denotes experimental conditions in which cells were transfected with a control plasmid.

Figure 4: Elongator affects tumorigenic potential of melanoma cells. A and **B.** Ability of Elp1 (A) or Elp3 (B)-depleted B16-F10 cells to form colonies in soft agar was examined. The indicated cells were seeded in agar-containing media, as described in the methods, and pictures were taken two weeks after seeding. The number of colonies observed in control B16-F10 cells was set to 100%, and the number of colonies obtained in other experimental conditions expressed relative to that. The figures show the data from a representative experiment performed in triplicates (mean values ± S.D.). **C**. Invasion of control or Elp1-depleted cells was evaluated by using a 3D cell culture system (described in the methods). On the top, pictures were taken three weeks after seeding. At the bottom, the number of colonies obtained in control cells was set to 100% and the number of colonies observed in other experimental conditions expressed relative to that. The figures show the data from a representative experiment performed in triplicates (mean values ± S.D.)

Figure 5: Elp5 and Elp6 are essential for migration and tumorigenicity of melanoma-derived cells. A. and **C**. Elp5 (A) or Elp6 (C) were depleted in B16-F10 cells by infection with two specific shRNAs (#1 and #2), as judged by qRT-PCR analysis. **B**. and **D**. Migration of control, Elp5 (B) or Elp6 (D)-depleted cells was assessed by wound healing assay. Pictures were taken at the indicated times. The quantification of the data is plotted. For each experimental condition, the width of the wound was set to 100% at time 0 and the width in other time points expressed relative to that. The

figure shows the data from a representative experiment performed in triplicates (mean values ± S.D.). **E**. and **F**. The number of colonies formed in soft agar was dramatically reduced in Elp5 (E) or Elp6 (F)-deficient versus control B16-F10 cells. The indicated cells were seeded in agar-containing media, as described in the methods. Pictures were taken two weeks after seeding. The number of colonies observed in control B16-F10 cells was set to 100% and the number of colonies obtained in Elp5 or Elp6-depleted cells expressed relative to that. The figure show the data from a representative experiment performed in triplicates (mean values ± S.D.).

Figure 6: Elp5 regulates cell migration of melanoma-derived cells as part of the Elongator complex. A. Schematic representation of full-length ELP5 and mutants tested for interaction with ELP1, ELP3 and ELP4. The Hap2 elong superfamily domain (described in (54)) is schematically illustrated. **B**. HEK293 cells were transfected with the indicated expression plasmids and cell extracts were subjected to anti-FLAG immunoprecipitations followed by an anti-ELP4 western blot (top panel). As inputs, FLAG expression constructs were detected in crude cell extracts by an anti-FLAG western blot analysis (bottom panel). **C**. HEK293 cells were transfected with the indicated expression plasmids and cell extracts were subjected to anti-FLAG immunoprecipitations followed by anti-ELP1 or -Myc western blots (top and second panel from the top). As inputs, FLAG- or Myc- expression constructs were detected in crude cell extracts by an anti-FLAG or anti-Myc western blot analysis (bottom panel) **D**. Wound healing assays were conducted with control, shRNA Elp5 B16-F10 cells or with shRNA Elp5 B16-F10 cells transfected with full length ELP5 or with the ELP5 mutant lacking the first 150 N-terminal amino acids ("ELP5-ΔN150"). A quantification of the data obtained is illustrated on the right. For each experimental condition, the width of the wound was set to 100% at time 0 and the width in other time points expressed relative to that. The figure shows the data from a representative experiment performed in triplicates (mean values ± S.D.). On the left, anti-FLAG western blots were carried out with protein extracts from the indicated cells collected at the end of the wound healing assay. "Mock" denotes experimental conditions in which cells were transfected with a control plasmid.

Figure 7: ELP5 connects ELP3 to ELP4. A and **B.** Control or shRNA ELP5 HEK293 cells were transfected with a control plasmid ("Mock") or a ELP4-FLAG (A) or FLAG-ELP3 (B) expression plasmid, as indicated. Cell extracts from the resulting cells were subjected to anti-FLAG immunoprecipitations followed by anti-ELP1 (A and B), -ELP3 (A and B), -FLAG (A) and -ELP4 (B) western blots. As inputs, ELP5 (A and B), ELP4 (B) or FLAG-expressing constructs (B) were detected in crude cell extracts by western blotting (bottom panels).

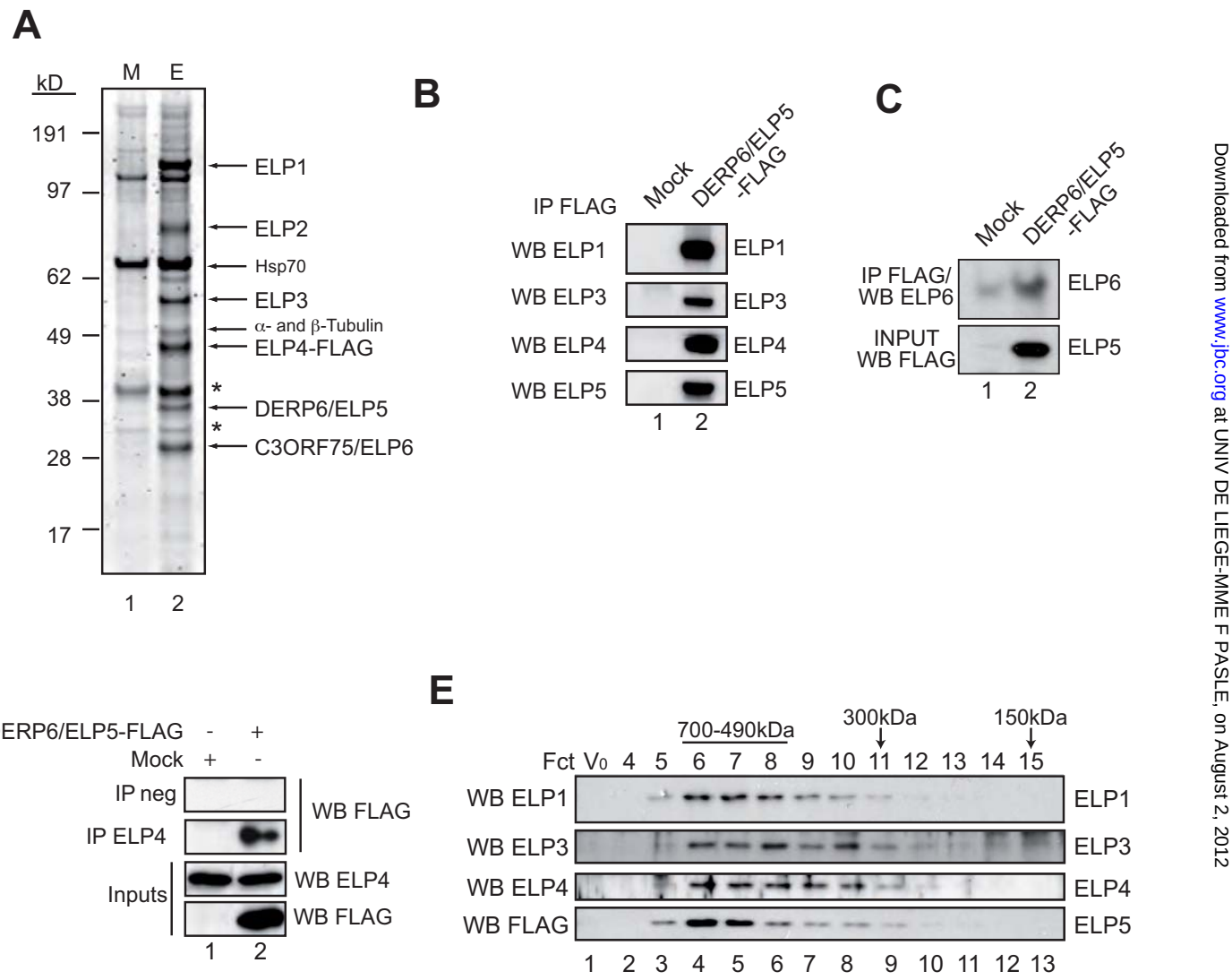

Figure 1

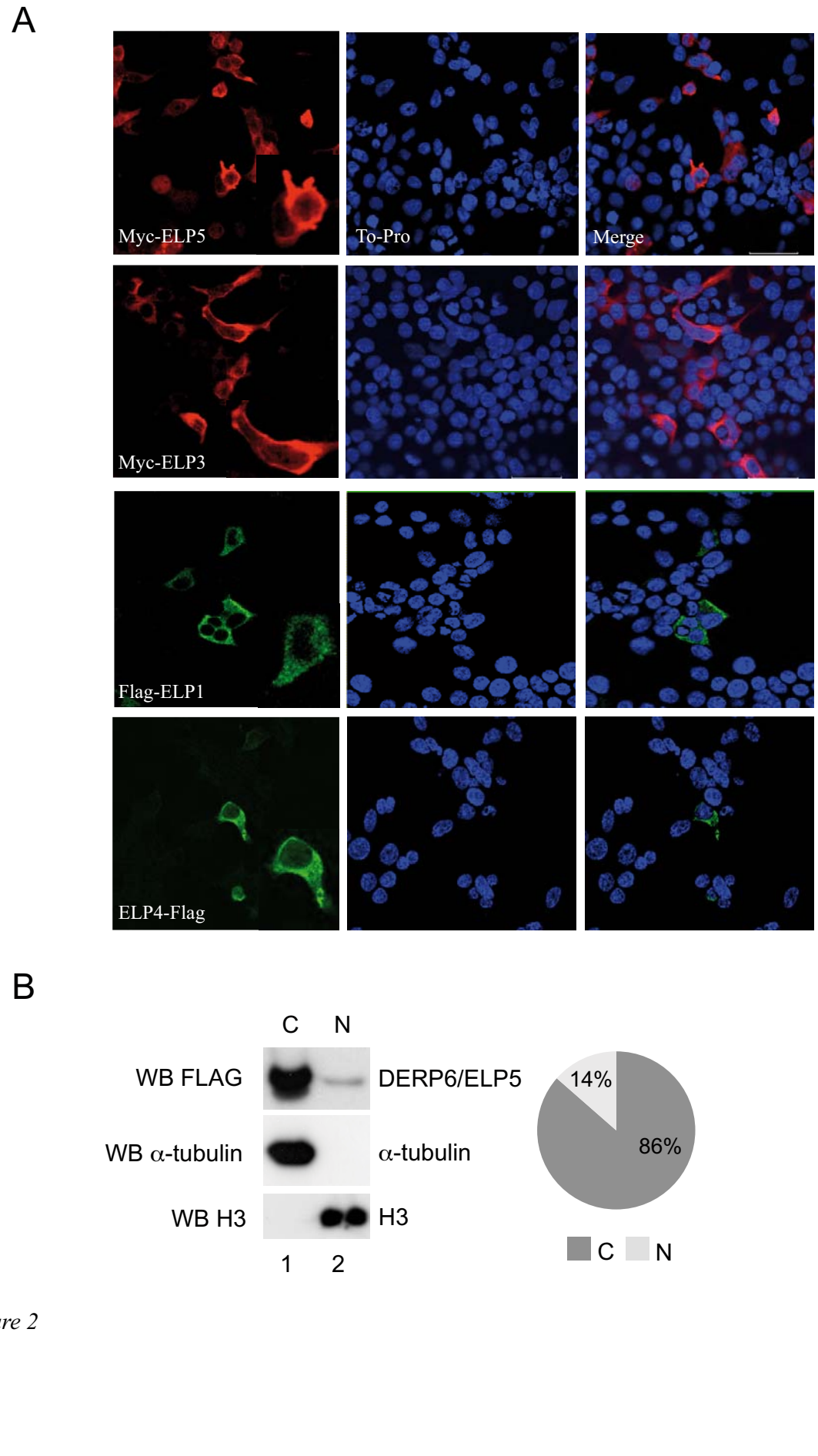

Figure 2

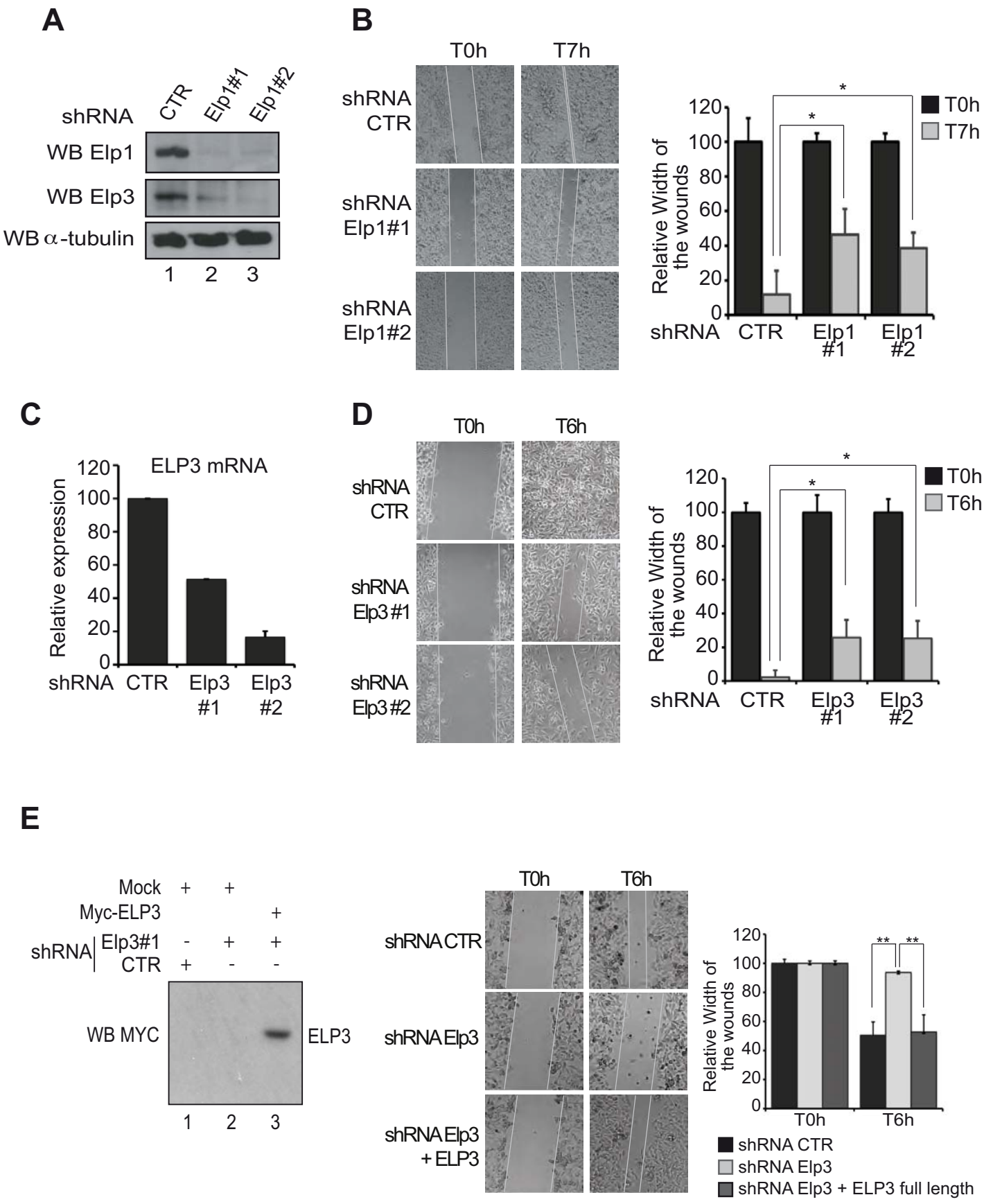

Figure 3

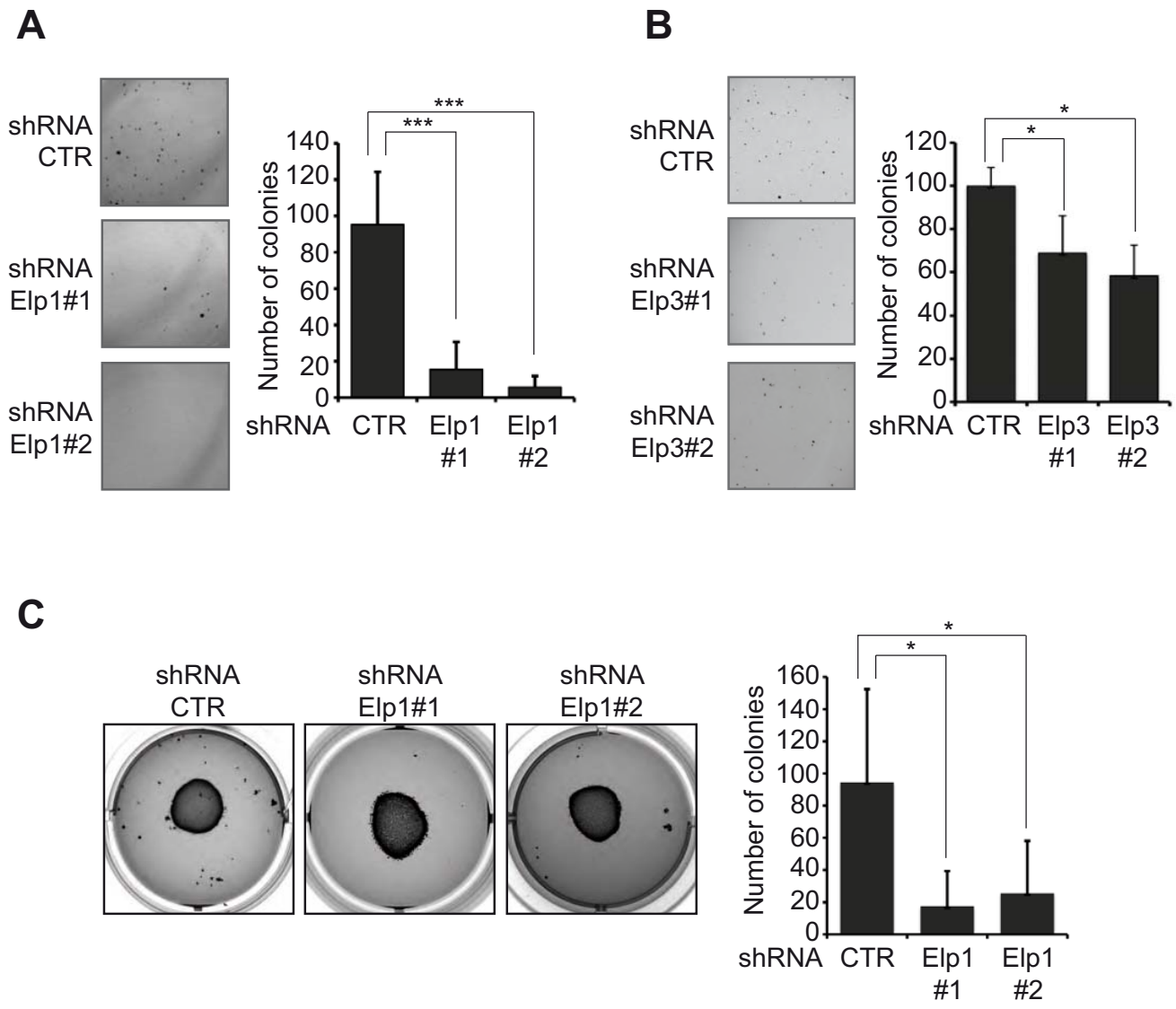

Figure 4

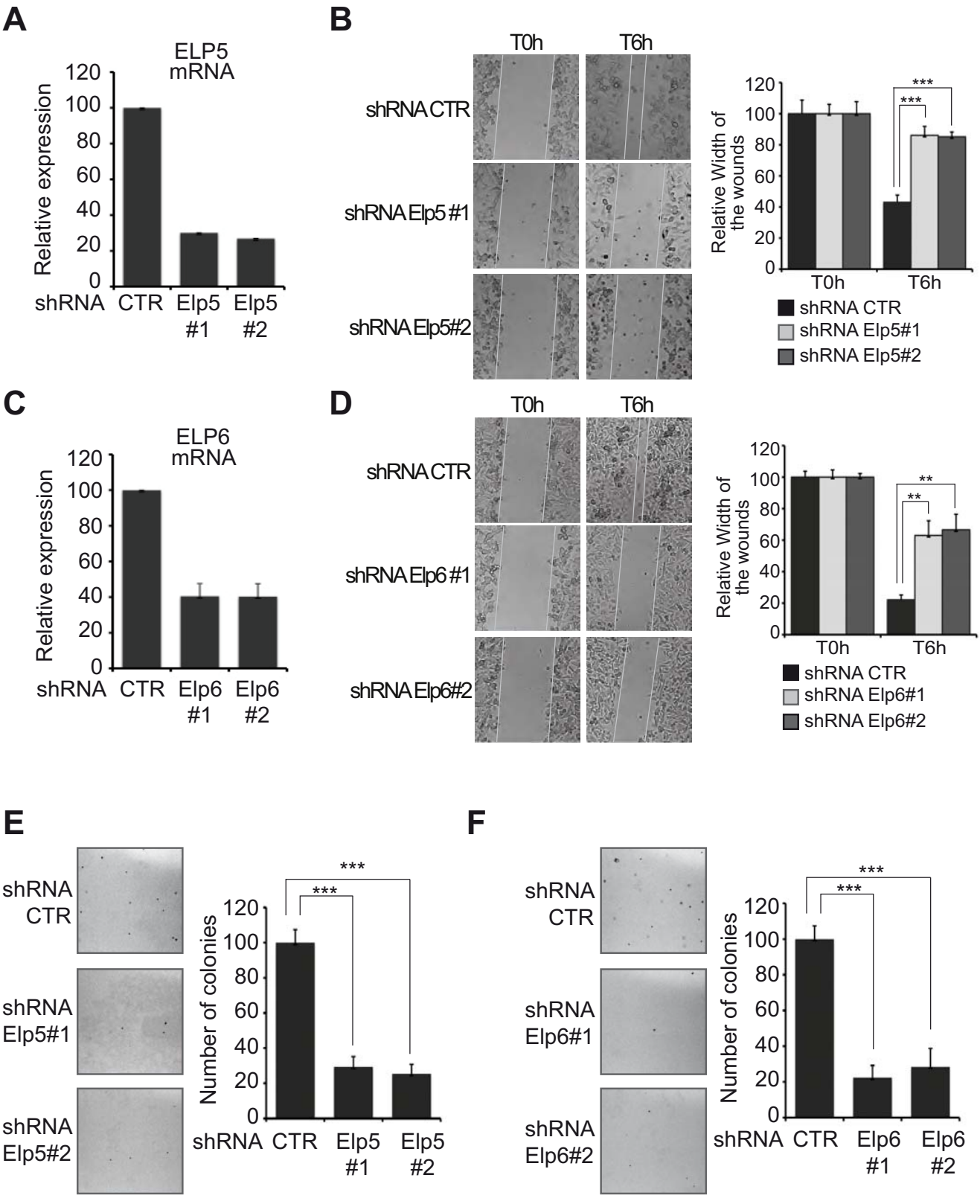

Figure 5

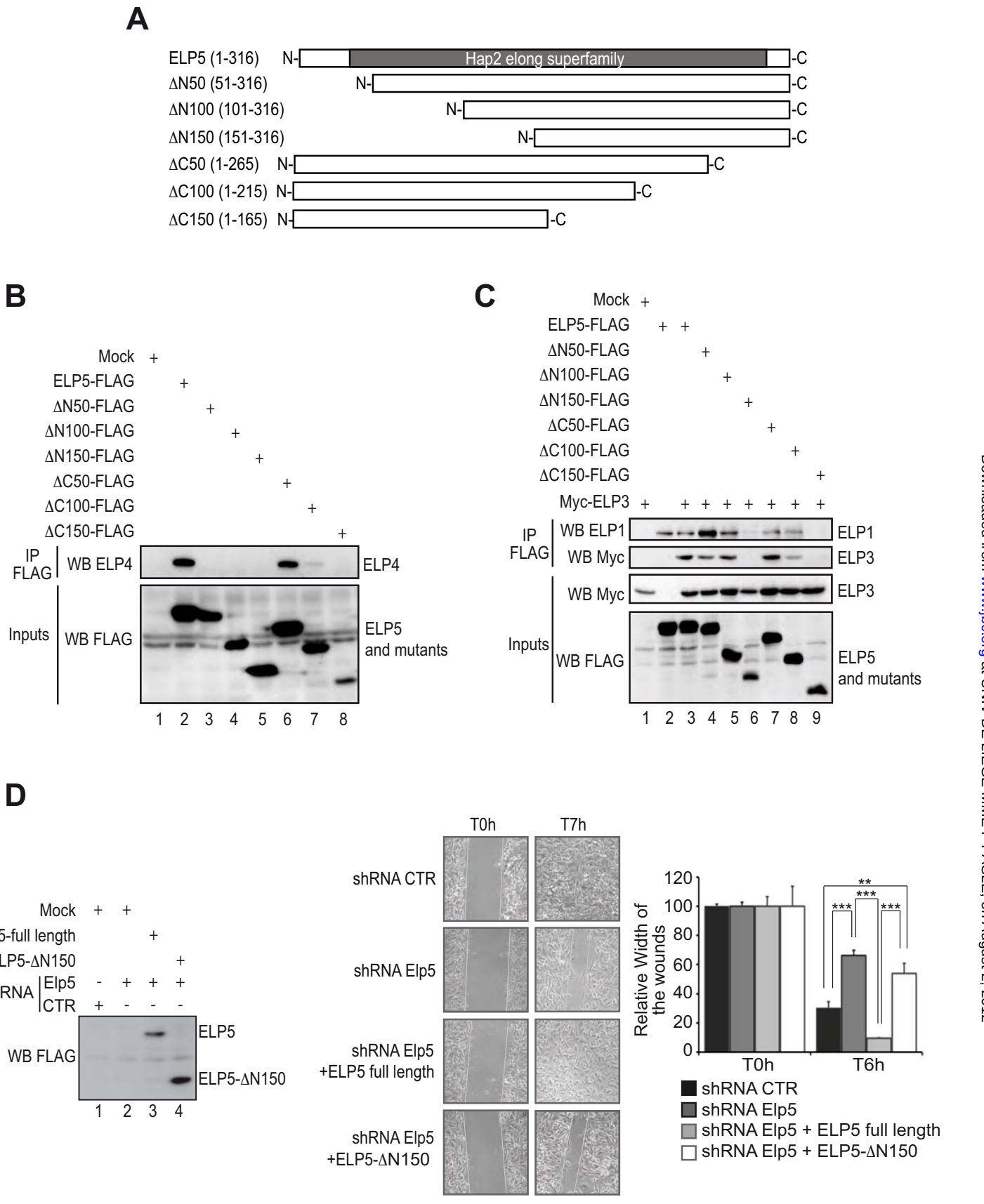

Figure 6

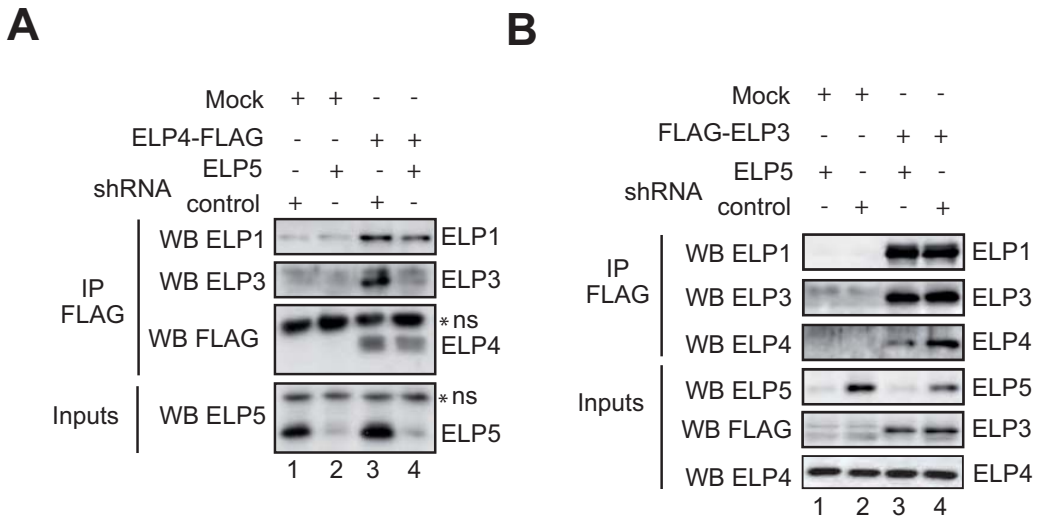

Figure 7

SUPPLEMENTARY FIGURES AND TABLES

Supplementary Figure 1: Identification of DERP6 and C3ORF75 by MS/MS. On the top, the peptide sequences and ion scores of both identified proteins are mentioned. At the bottom, DERP6 and C3ORF75 protein sequences. Sequenced peptides are highlighted in red.

Protein name	SwissProt Access number	Mass Protein (Da)	Peptide Sequences	Start - End	Mass Observed (Da)	Mr (expt) (Da)	Mr (calc) (Da)	Delta (Da)	Ion Sore	Expect
Dermal papilla-derived protein 6 **DERP6**	**Q8TE02**	**35219**	R.EGFDSDINNR.L K.TEEAFPGGPLGALR.A	70 – 79 95 – 108	583.7800 707.9000	1165.5454 1413.7854	1165.5000 1413.7252	0.0455 0.0602	56 52	6.3^{e}-04 1.5^{e}-03
UPF0405 protein **C3ORF75**	**Q0PNE2**	**30116**	K.GMSPAVL.- + Oxidation (M) K.LTLLCDAK.T K.LGVSLTMAR.E + Oxidation (M) R.ATVCWELK.G R.AEGLATGFCR.D R.GQLVFLEGLK.S R.DQSFTYQYK.I K.SAVDVVFQAQK.E	260 – 266 21 – 28 68 – 76 168 – 175 210 – 219 79 – 88 240 – 248 89 – 99	690.3800 467.3000 482.3200 502.7700 541.2500 552.5800 590.3500 596.5000	689.3727 932.5854 962.6254 1003.5254 1080.4854 1103.1454 1178.6854 1190.9854	689.3418 932.5001 962.5219 1005.4953 1080.5022 1102.6386 1178.5244 1190.6295	0.0309 0.0854 0.1036 1.9699 0.0168 0.5068 0.1610 0.3559	14 45 82 7 57 66 49 96	30 0.019 3.2^{e}-06 1.7^{e}+02 1.8^{e}-03 1.5^{e}-04 5.6^{e}-03 1.1^{e}-07

DERP6

1 MTPSEGARAG TGRELEMLDS LLALGGLVLL RDSVEWEGRS LLKALVKKSA
51 LCGEQVHILG CEVSEEEFR**E GFDSDINNR**L VYHDFFRDPL NWSK**TEEAFP**
101 **GGPLGALR**AM CKRTDPVPVT IALDSLSWLL LRLPCTTLCQ VLHAVSHQDS
151 CPGDSSSVGK VSVLGLLHEE LHGPGPVGAL SSLAQTEVTL GGTMGQASAH
201 ILCRRPRQRP TDQTQWFSIL PDFSLDLQEG PSVESQPYSD PHIPPVDPTT
251 HLTFNLHLSK KEREARDSLI LPFQFSSEKQ QALLRPRPGQ ATSHIFYEPD
301 AYDDLDQEDP DDDLDI

C3ORF75

1 MFVELNNLLN TTPDRAEQGK **LTLLCDAK**TD GSFLVHHFLS FYLKANCKVC
51 FVALIQSFSH YSIVGQK**LGV SLTMAR**ER**GQ LVFLEGLKSA VDVVFQAQK**E
101 PHPLQFLREA NAGNLKPLFE FVREALKPVD SGEARWTYPV LLVDDLSVLL
151 SLGMGAVAVL DFIHYCR**ATV CWELK**GNMVV LVHDSGDAED EENDILLNGL
201 SHQSHLILR**A EGLATGFCR**D VHGQLRILWR RPSQPAVHR**D QSFTYQYK**IQ
251 DKSVSFFAK**G MSPAVL**

Supplementary Figure 2: MS/MS spectra for one of the peptides sequenced from DERP6 (A) and C3ORF75 (B).

(A)

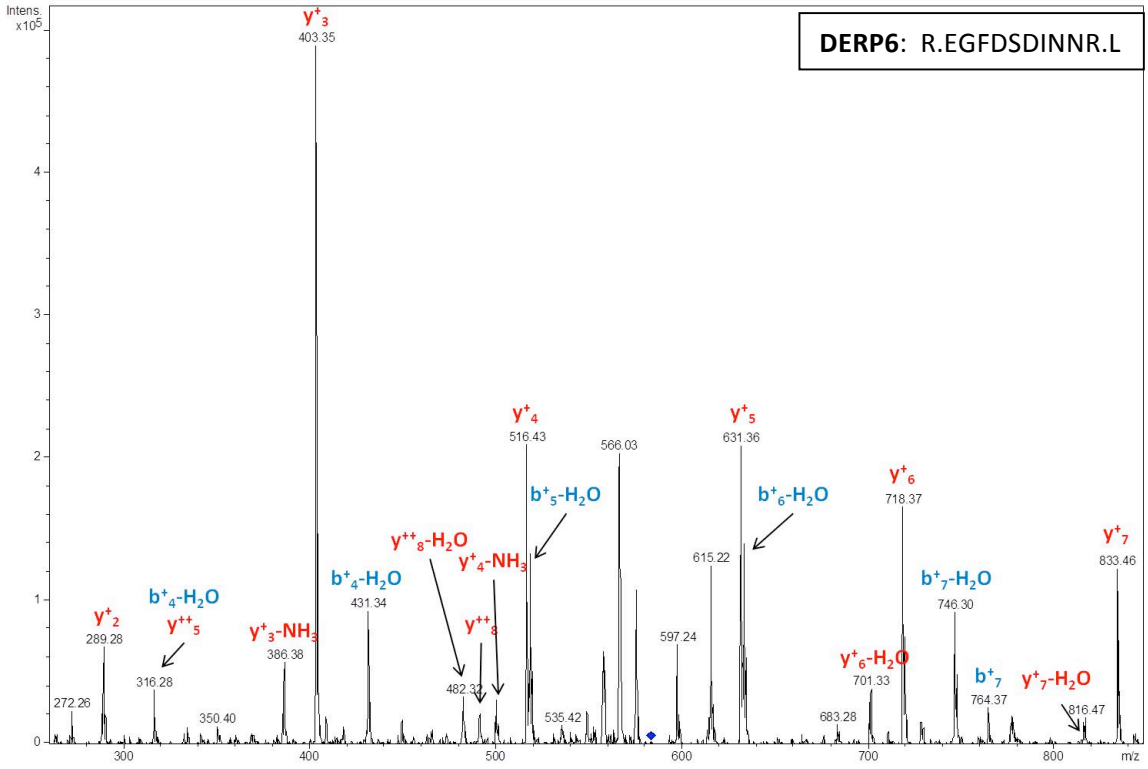

(B)

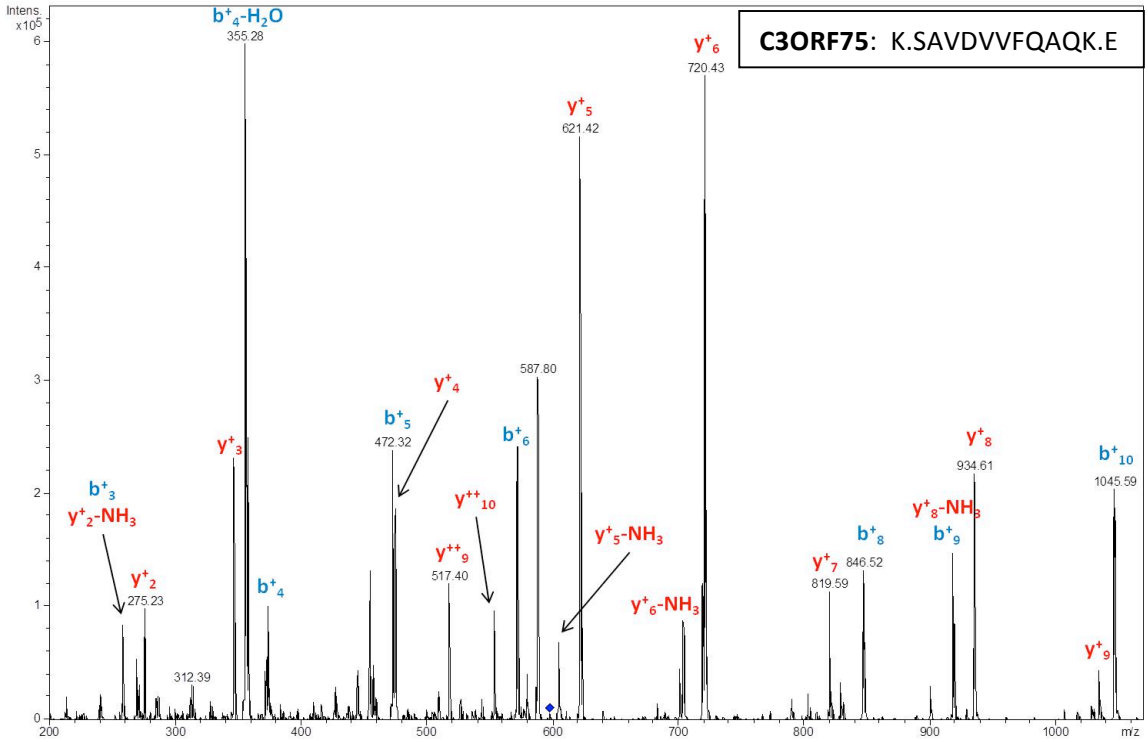

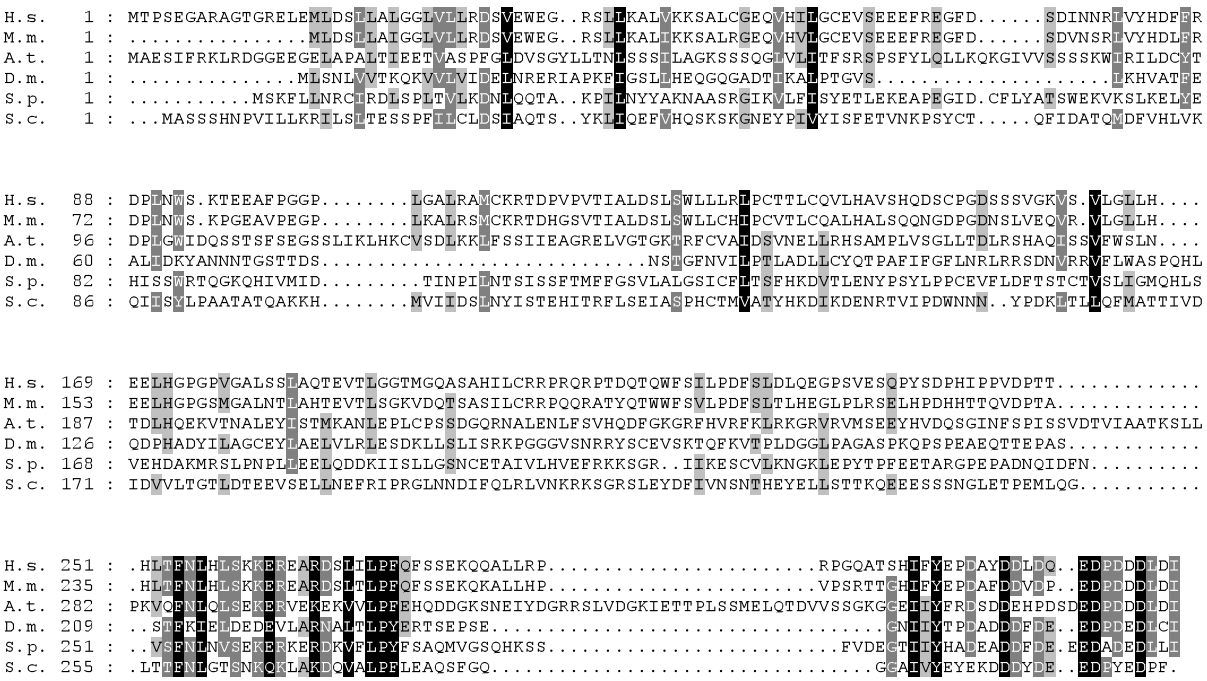

Supplementary Figure 3: Multiple sequence alignment of DERP6/ELP5 and its homologues from other species using ClustalW2 (1). *H.s.*, *Homo sapiens*; *M.m.*, *Mus musculus*; *A.t.*, *Arabidopsis thaliana*; *D.m.*, *Drosophila melanogaster*; *S.p.*, *Schizosaccharomyces pombe*; *S.c.*, *Saccharomyces cerevisiae*. 60% conserved residues are shaded in light gray, 80% conserved residues are shaded in dark gray and identical residues are shaded in black. Similarity groups' option is enabled. Homology between human DERP6/ELP5 and *S. cerevisiae* Elp5 is 15% identical and 29% similar. Homology comparison of different homologues ranges from 8% identical/25% similar (*A. thaliana* and *S. cerevisiae*) to 71% identical/80% similar (*H. sapiens* and *M. musculus*).

Reference:

1. Larkin, M. A., Blackshields, G., Brown, N. P., Chenna, R., McGettigan, P. A., McWilliam, H., Valentin, F., Wallace, I. M., Wilm, A., Lopez, R., Thompson, J. D., Gibson, T. J., and Higgins, D. G. (2007) *Bioinformatics* **23**, 2947-2948

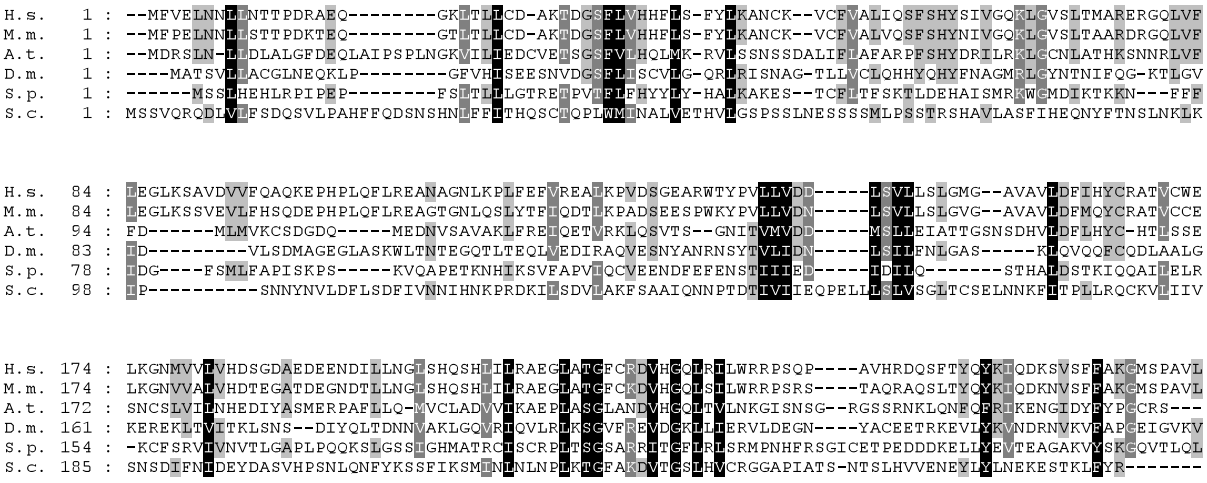

Supplementary Figure 4: Multiple sequence alignment of C3ORF75/ELP6 and its homologues from other species using ClustalW2 (1). *H.s.*, *Homo sapiens*; *M.m.*, *Mus musculus*; *A.t.*, *Arabidopsis thaliana*; *D.m., Drosophila melanogaster; S.p., Schizosaccharomyces pombe; S.c., Saccharomyces cerevisiae*. 60% conserved residues are shaded in light gray, 80% conserved residues are shaded in dark gray and identical residues are shaded in black. Similarity groups' option is enabled. Homology between human C3ORF75/ELP6 and *S. cerevisiae* Elp6 is 9% identical and 25% similar. Homology comparison of different homologues ranges from 8% identical/26% similar (*M. musculus* and *S. cerevisiae*) to 80% identical/90% similar (*H. sapiens* and *M. musculus*).

Reference:

1. Larkin, M. A., Blackshields, G., Brown, N. P., Chenna, R., McGettigan, P. A., McWilliam, H., Valentin, F., Wallace, I. M., Wilm, A., Lopez, R., Thompson, J. D., Gibson, T. J., and Higgins, D. G. (2007) *Bioinformatics* **23**, 2947-2948

Supplementary Table 1: shRNA sequences used in this study

shRNA and species	Tracking number	Sequence
Ctrl	SHC002	non-mammalian sequence
Elp1#1 mus musculus	TRCN0000088775	CGCTGAGTGAAGTGGTACAAA
Elp1#2 mus musculus	TRCN0000088773	CCTCAGTTCCTGTTGTTCATA
Elp3#1 mus musculus	TRCN0000039309	CGGAGAGATTATGTTGCCAAT
Elp3#2 mus musculus	TRCN0000039311	GCACAAGAAATTATTACCGAA
Elp5#1 mus musculus	TRCN0000192282	CCTTGTCCTTTGTTACTTTGT
Elp5#2 mus musculus	TRCN0000189577	CCCTGTGTTACACTCTGTCAA
ELP5 homo sapiens	TRCN0000130483	GCCCAGAACCATCTTTCTATT
Elp6#1 mus musculus	TRCN0000267114	CTTCTACCTGAAAGCTAATTG
Elp6#2 mus musculus	TRCN0000267116	TGTCCAGTCCTTCAGCCATTA

Supplementary Table 2: Oligonucleotide sequences used to assess mRNA expression through qRT-PCR analysis

Name and species	Forward primer	Reverse primer
GAPDH mus musculus	TGATGACATCAAGAAGGT GGTGAAG	TCCTTGGAGGCCATGTAGGCCAT
ELP3 mus musculus	AGGACCTGACTCCGATTTTG	CTCTCATGGAAGTTGGCTCA
ELP5#1 mus musculus	CATTGCCCTTGACTCTCTCA	CAGAGCATGTAGGGCTTGAC
ELP5#2 mus musculus	GTCTCCTGAAGGCTCTTATC	TCTGAAGAGGTCATGGTAAAC
ELP6#1 mus musculus	CCGGAACTCAACAACCTTCT	AGCGTCACAGAGGAGAGTCA
ELP6#2 mus musculus	GTCTGCTTTGTGGCACTTGT	AGAGGACTTGAGACCCTCCA